Supporting Information

A novel metal-organic framework of Co-hemin for portable and visual colorimetric detection of 2,4-Dichlorophenoxyacetic Acid

Jintao Yi*[a], Xianqin Han[a], Qi Zhu[a], Lingli Wu[a], Youtan Wang[a], Jun Xue*[a], Xiaoqi Lai*[a], Hui Zhou*[ab]

[a.]Key Laboratory of Organo-Pharmaceutical Chemistry of Jiangxi Province, Gannan Normal University, Ganzhou 341000, P. R. China

[b.]Guangdong Provincial Key Laboratory of Research and Development of Natural Drugs, and School of Pharmacy, Guangdong Medical University, Dongguan 523808, PR China

E-mail: yistarthappy@163.com; Fax: (+86)797-8393536; Tel: +86-797-8393536

Experimental section

1.1 Materials and reagents

Cobalt chloride hexahydrate, hemin, acetic acid, sodium acetate, 2,4-dichlorophenoxyacetic acid (2,4-D), alkaline phosphatase (ALP), 3, 3′, 5, 5′-tetramethylbenzidine (TMB), chlorpyrifos (CPF), dichlorphos (DDVP), trichlorfon (TRC), carbendazim (MBC), triazolone (TDM) and fenvalerate (FV) were bought from Sigma-Aldrich. Ascorbic acid (AA) and ascorbic acid-2-phosphate trisodium salt (AAP) were purchased from Sangon Biological Engineering Technology & Services Company Ltd. (Shanghai, China). All other reagents were of analytical grade. Ultrapure water was from a Millipore Milli-Q water purification system (Billerica), which had an electric resistance >18.25 MΩ.

1.2 Apparatus

The UV spectra were obtained from the UV-2700 UV-visible spectrophotometer (Shimadzu Instrument, Inc., Japan). The crystal phases of particles were measured on scanning electron microscope (Bruker, Germany). The Fourier transform infrared (FT-IR) spectroscopy were detected at spectrometer. The crystal phases of particles were determined by D8-advance X-ray diffraction (Bruker, Germany). The thermo gravimetric analysis (TGA) was measured from the TG 209 F1 Libra thermal gravimetric analyzer (Netzsch, Germany). The X-ray photoelectron spectroscopy (XPS) was measured on Thermo Scientific K-Alpha+ by using Al Ka irradiation as the light source and applying the C 1s signal (284.8 eV) for spectrum cal.

1.3 The detection of AA by Co-hemin

In the assay of AA detection, 1.95 μL of AA (10 mM), 15 μL of Co-hemin (1 mg/mL), 37 μL of HAc-NaAc buffer (0.4 M, pH 4.5), 10 μL of TMB solution (5 mM) and 86.05 μL of sterile water were mixed and incubated for 10 min at 25 ℃. Then the absorbance at 652 nm was detected.

1.4 The detection of ALP by Co-hemin

In the assay of ALP detection, 5 μL of ALP (810 U/L) and 10 μL of AAP (10 mM) were reacted for 20 min, next sequentially adding of TMB solution (10 μL, 5 mM), HAc-NaAc buffer (37 μL, 0.4 M, pH 4.5), Co-hemin (15 μL, 1 mg/mL) and sterile water (73 μL), the obtained mixture solution were incubated for 10 min at 25 ℃.Then the absorbance at 652 nm was detected.

Table S1. A comparison of the analytical performance of Co-hemin using other sensors for 2,4-D detection.

Materials	Linear range for 2,4-D (μg/mL)	Detection limit for 2,4-D (ng/mL)	Reference
QD@SiO_2@NBD@MIPs	0.09-22.1	31	1
Fe_3O_4-PANI	0.3-0.6	46	2
PPy-GC electrode	0.2-2.2	184	3
CDs/CoOOH	0-15	100	4
Co-hemin	0.1-240	33	This work

Table S2. Results of the detection of 2,4-D in serum and tap water.

Sample	Added (μg/mL)	Colorimetry			HPLC		
		Founded (μg/mL)	Recovery (%)	RSD (%, n=3)	Founded (μg/mL)	Recovery (%)	RSD (%, n=3)
Serum	40	45.2	113	2.5	39.2	98	2.3
	80	89.5	111.8	1.1	89.5	111.9	3.1
	120	109.8	91.5	3.6	120.4	100.3	1.8
	140	126.9	90.7	4.4	142.4	101.7	2.6
Tap water	40	40.6	101.5	2.2	35.1	87.8	3.3
	80	71.5	89.4	3.5	89.5	111.9	1.5
	120	113.6	94.7	2.9	125.3	104.4	2.8
	140	130.9	93.5	4.3	136.6	97.6	1.9

Table S3. Results of the detection of 2,4-D in rice and apple.

Sample	Added (μg/mL)	Colorimetry			HPLC		
		Founded (μg/mL)	Recovery (%)	RSD (%, n=3)	Founded (μg/mL)	Recovery (%)	RSD (%, n=3)
rice	2	2.2	110	1.2	2.1	105	1.3
	5	4.7	94	2.3	4.5	90	2.1
	8	7.1	88.8	1.8	7.5	93.8	2.8
	12	12.8	106.7	3.2	12.8	106.7	1.6
apple	2	2.3	115	3.2	1.7	85	2.3
	5	4.4	88	2.5	4.4	88	1.5
	8	8.3	103.8	2.0	8.8	110	2.0
	12	11.2	93.3	1.3	12.2	101.7	1.9

Fig. S1 The UV-vis absorbance spectrum of Co-hemin MOF.

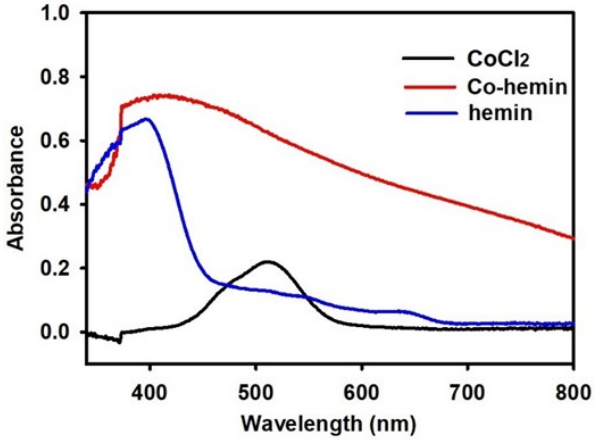

Fig. S2 The elemental mapping images and SEM images of Co-hemin.

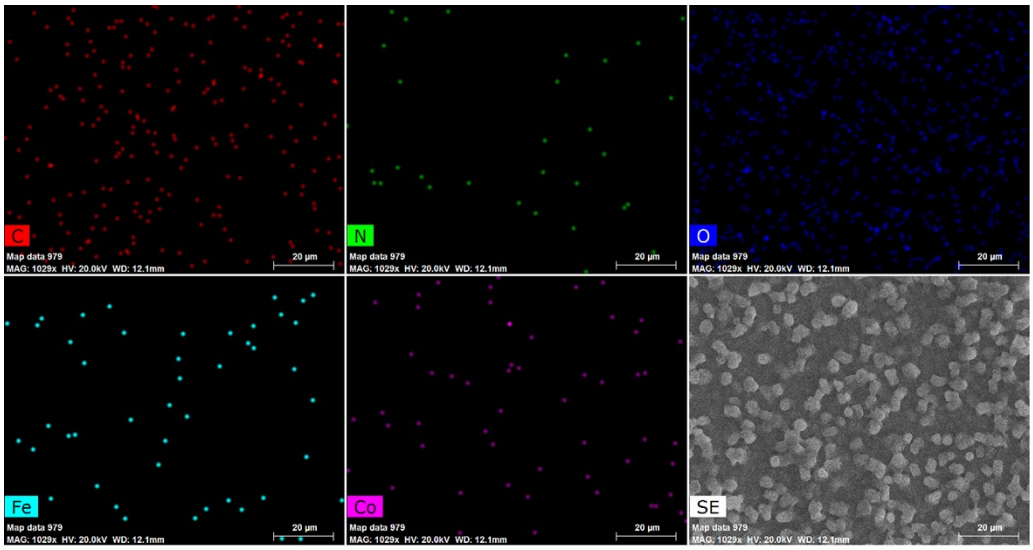

Fig. S3 The XPS spectra of Co-hemin. (A) Survey spectrum, (B) C 1s, (C) N 1s, (D) O 1s, (E) Fe 2p, (F) Co 2p.

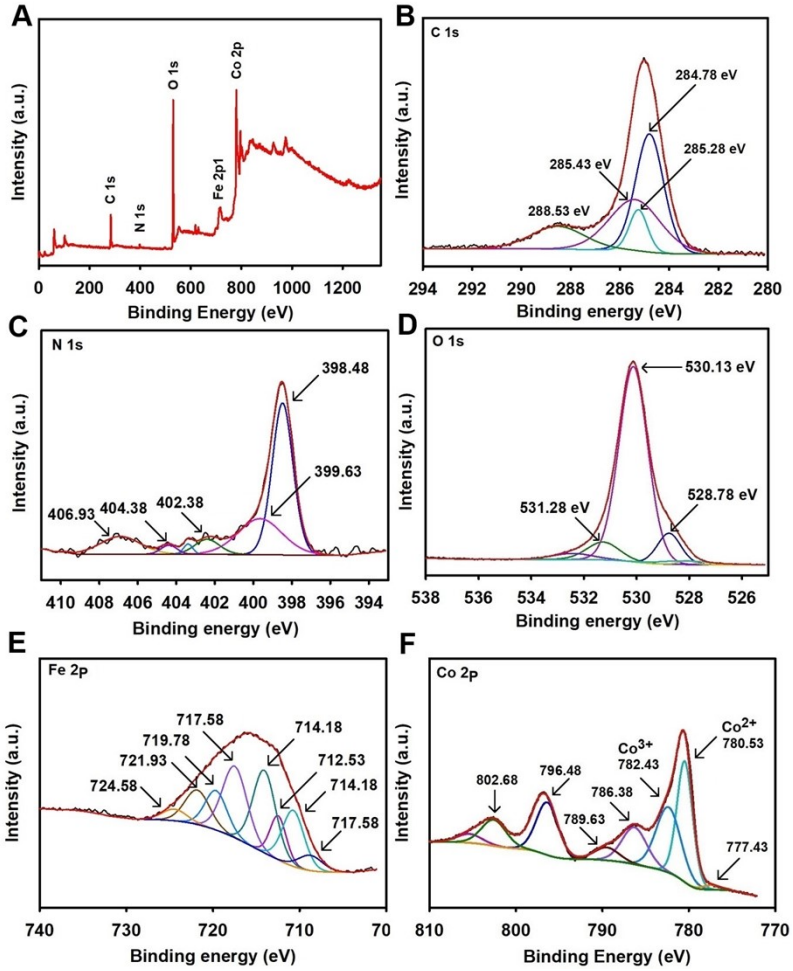

Fig. S4 The TGA of Co-hemin.

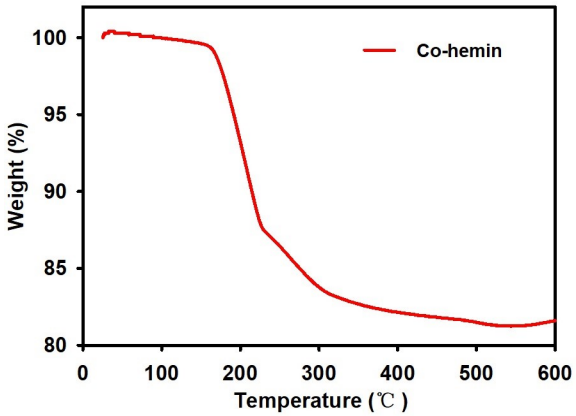

Fig. S5 The oxidase-like activities of Co-hemin and hemin for colorimetric assay.

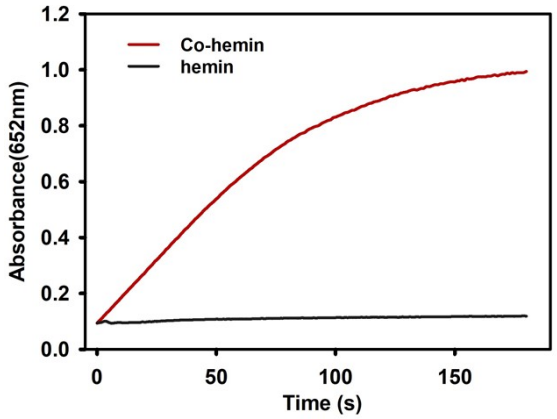

Fig. S6 The stability of Co-hemin in different concentrations of AA.

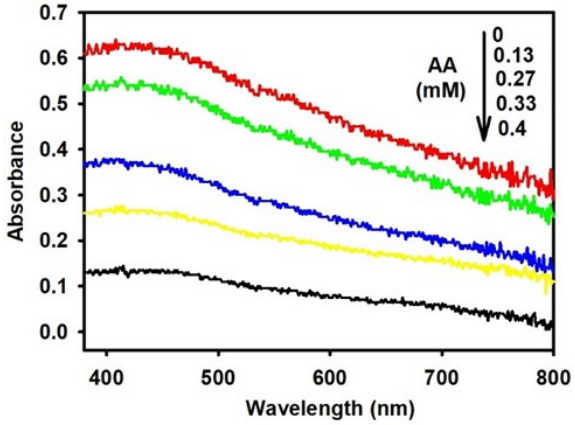

Fig. S7 The Co-hemin MOF degraded by AA in the presence of TMB, (A) The UV-vis absorbance spectrum. (B) The relationship between the UV absorbance and the concentration of AA. Insert: the corresponding linear relationship. (C) The corresponding color images and the RGB calculations. Error bars represented the standard deviation and were obtained from three parallel experiments.

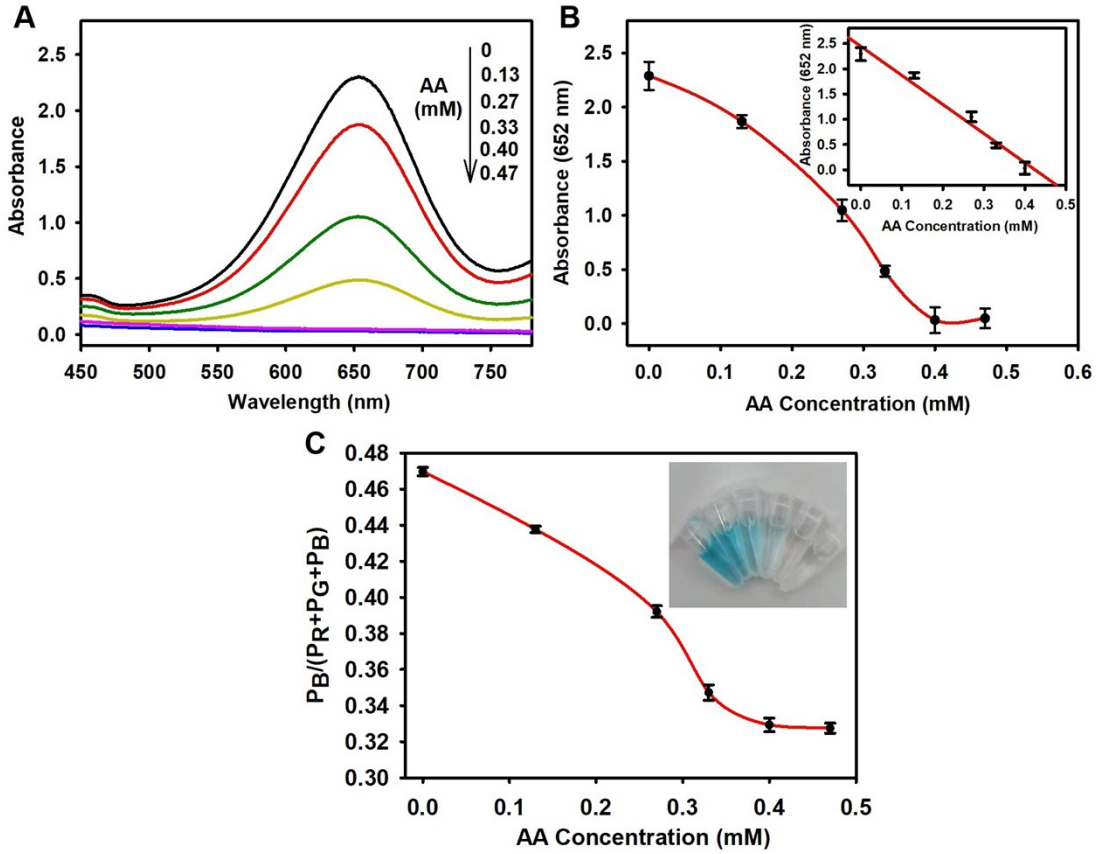

Fig. S8 The time optimization of ALP detection. Error bars were obtained from three parallel experiments and represented the standard deviation.

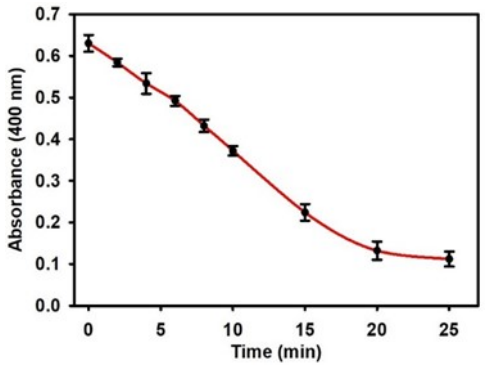

Fig. S9 The detection of ALP by Co-hemin. (A) The UV-vis absorbance spectrum. (B) The relationship between the UV absorbance and the concentration of ALP. Insert: the corresponding linear relationship. (C) The corresponding color images and the RGB calculations. Error bars were obtained from three parallel experiments and represented the standard deviation.

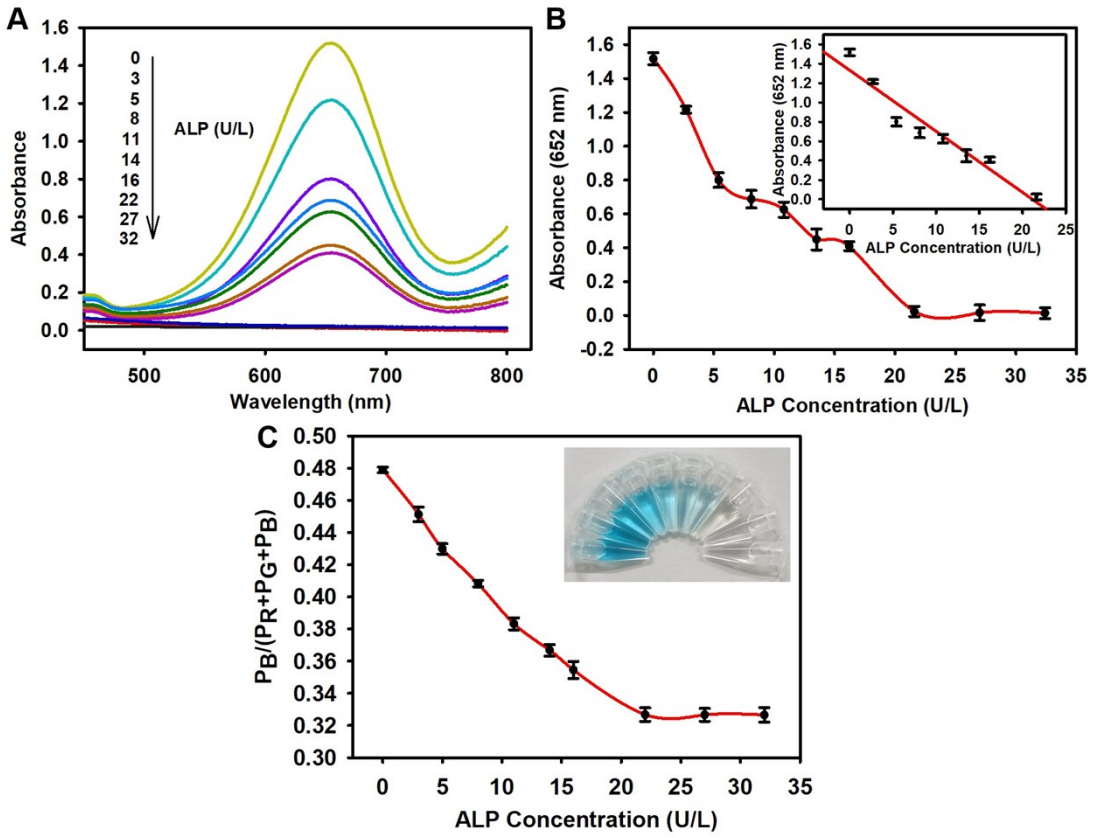

Fig. S10 The colorimetric detection of 2,4-D by Co-hemin on absorbent paper, (a) TMB, (b) Co-hemin, (c) AAP, (d) ALP, (e) 2,4-D, (f) Co-hemin + AAP, (g) Co-hemin + ALP, (h) Co-hemin + AAP + ALP, (i) Co-hemin + AAP +ALP + 2,4-D, (j) Co-hemin + AA.

Fig. S11 The corresponding RGB calculations of the colorimetric image of 2,4-D detection. Error bars represented the standard deviation of three parallel experiments.

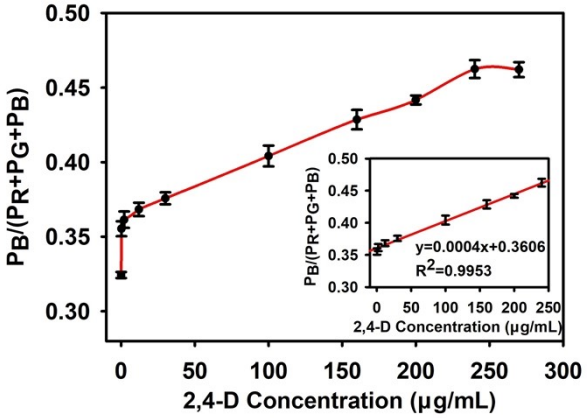

Fig. S12 The specificity of 2,4-D detection. (A) The UV-vis absorbance. (B) The corresponding colorimetric images. (C) The corresponding RGB calculations. Error bars were obtained from three parallel experiments and represented the standard deviation.

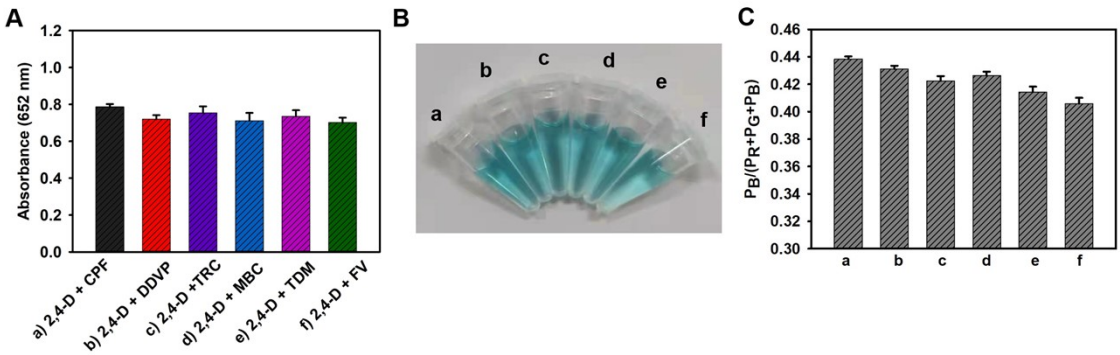

Fig. S13 The "INHIBIT" logical gate by using ALP and Co-hemin as inputs and the absorption at 652 nm as output. (A) Kinetics curves for monitoring the TMB catalytic oxidation. (B) The histogram of the "INHIBIT" logical gate. Error bars represented the standard deviation of three parallel experiments. (C) The schematic diagram of the "INHIBIT" logical gate.

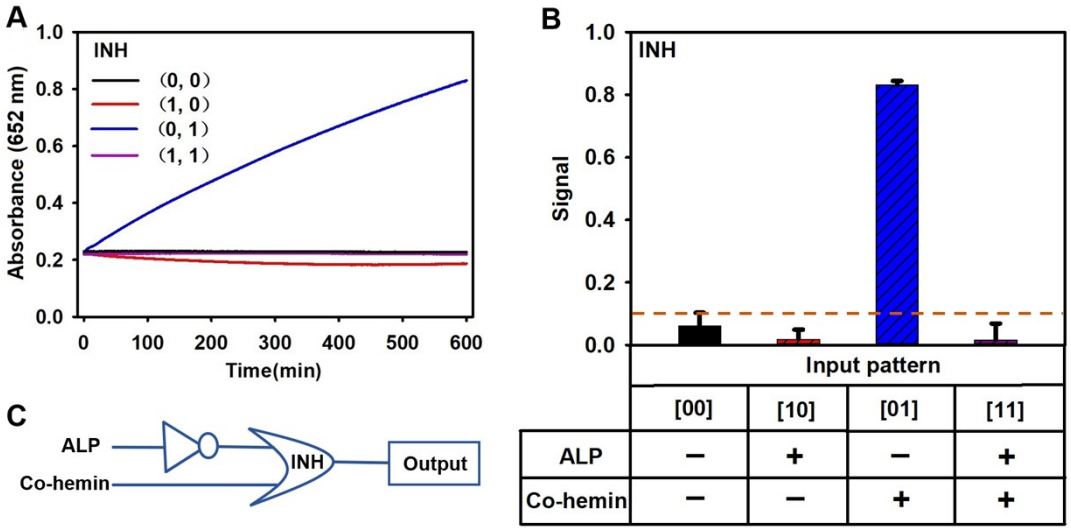

Fig. S14 The "NOR" logical gate by using ALP and AA as inputs and the absorption at 652 nm as output. (A) Kinetics curves for monitoring the TMB catalytic oxidation. (B) The histogram of the "NOR" logical gate. Error bars represented the standard deviation of three parallel experiments. (C) The schematic diagram of the "NOR" logical gate.

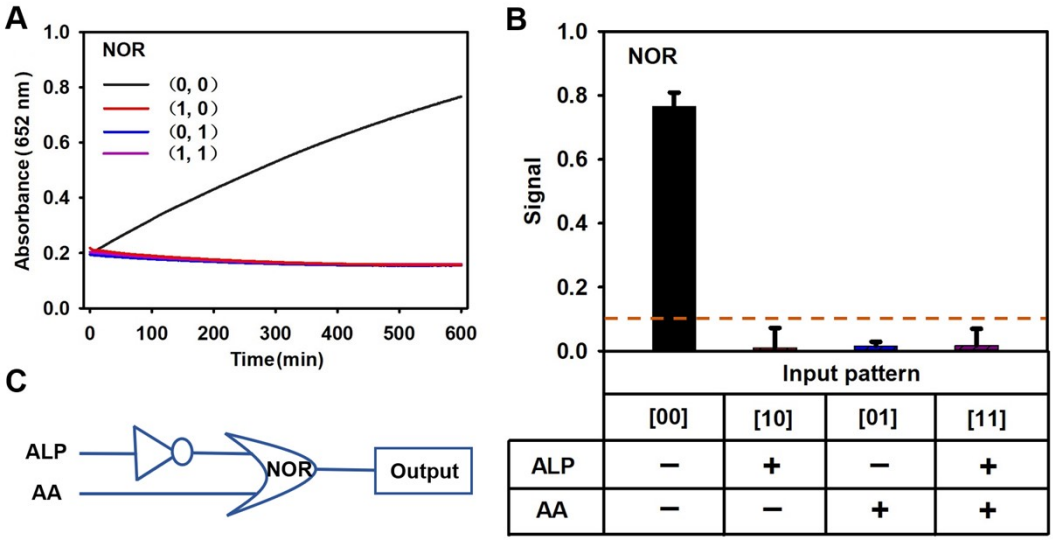

Reference

1 Wang X. Y., Yu J. L., Wu X. Q., Fu J. Q., Kang Q., Shen D. Z., Li J. H. and Chen L. X., *Biosensors and Bioelectronics*, 2016, **81**, 438-444.

2 Goswami B. and Mahanta D., *ACS Omega*, 2021, **6**, 17239-17246.

3 Xie C. G., Gao S., Guo Q. B. and Xu K., *Microchim Acta.*, 2010, **169**, 145-152.

4 Su D. D., Han X. S., Yan X., Jin R., Li H. X., Kong D. S., Gao H., Liu F. M., Sun P. and Lu G. Y., *Anal Chem.*, 2020, **92**, 12716-12724.